INFLUENCE OF FRICTION CHARACTERISTIC ON THE PERFORMANCE OF CHAIN CVT DRIVES

Nilabh Srivastava

106 EIB, Flour Daniel Building, Department of Mechanical Engineering Clemson University
Clemson SC 29634, USA
tel.:+1 864 6502324, fax: +1 864 6564435, e-mail: snilabh@clemson.edu

Tmtiaz Haque

106 EIB, Flour Daniel Building, Department of Mechanical Engineering Clemson University
Clemson SC 29634, USA
Tel.:+1 864 6565628, fax: +1 864 6564435, e-mail: imtiaz. haque@clemson.edu

Abstract

A continuously variable transmission (CVT) is an emerging automotive transmission technology that offers a continuum of gear ratios between desired limits. A chain CVT falls under the category of friction-limited drives as its performance and torque capacity rely significantly on the friction characteristic of the contact patch between the chain and the pulley. The present research focuses on developing models to understand the influence of different friction characteristics on the dynamic performance of a chain CVT drive. Since the friction characteristic of the contact patch may vary in accordance with the loading and design configurations, it is crucial to study the influence of friction characteristic on the performance of a CVT. A detailed planar multibody model of a chain CVT is developed in order to accurately capture the dynamics characterized by the discrete structure of the chain, which causes polygonal excitations in the system. Friction between the chain link and the pulley sheaves is modeled using different mathematical models which account for different loading scenarios. The mathematical models, the computational scheme, and the results corresponding to different loading scenarios are discussed. The results discuss the influence of friction characteristics on the dynamic performance, the axial force requirements, and the torque transmitting capacity of a chain CVT drive.

Keywords: *continuously variable transmission, CVT, chain, friction characteristics, stribeck, pulley flexibility, lubrication*

1. Introduction

Over the past few decades, continuously variable transmissions (CVTs) have aroused a great deal of interest in the automotive sector due to their potential of lower emissions and better performance. A CVT is an emerging automotive transmission technology that offers an infinite number of gear ratios between two limits, which consequently allows better matching of the engine operating conditions to the variable driving scenarios. A CVT offers potential advantages over the conventional automatic and manual transmissions, chiefly: higher engine efficiency, better fuel economy, low cost, and infinite gear ratios with fewer parts. Today several auto manufacturers, such as Honda, Toyota, Ford, Nissan, etc., are already keen on exploiting the various advantages of a CVT in a real production vehicle.

A CVT comprises two variable diameter pulleys kept at a fixed distance apart and connected by a power-transmitting device like belt or chain with one of the sheaves on each pulley being movable. The belt/chain can undergo both radial and tangential motions, depending on the loading conditions and the axial forces applied to the pulley sheaves. The pulley on the engine side is called the driver pulley and the one on the final drive side is called the driven pulley.

Figure 1 depicts the chain structure and the basic configuration of a chain CVT drive. A

rocker-pin chain consists of plates and rocker pins, as depicted in the figure. All plates and pins transmit tractive power. The plates also prevent rocking of the pins by orienting them perpendicular to the direction of motion of the chain. Owing to the discrete structure of a chain, the contact forces between the pins and the pulleys are discretely distributed. Consequently, impact-related vibrations occur as chain links enter and leave the pulley. These excitation mechanisms, which are related to the polygonal action of chain links, significantly influence the performance of a chain CVT drive.

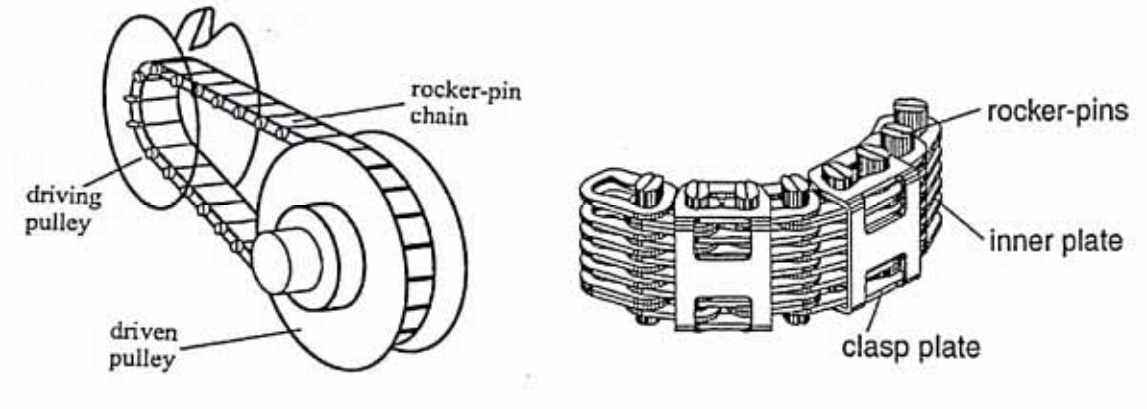

Fig. 1. Chain CVT and Chain Link Configuration [12]

A chain CVT falls under the category of friction-limited drives as its performance and torque capacity rely significantly on the friction characteristic of the contact patch between the chain and the pulley. The torque capacity of a friction-driven CVT (i.e. belt or chain CVT) is limited by the strength of the belt or chain and the ability to withstand friction wear between the source and transmission medium. A sundry of research is being conducted on different aspects of a CVT, e.g. performance, slip behavior, efficiency, configuration design, loss mechanisms, vibrations, etc [5,7,9-11]. Srnik and Pfeiffer [12] studied the dynamic behavior of a CVT chain drive for high-torque applications. They developed a planar model of chain CVT with three-dimensional contact between chain link and pulley. The work dealt with multi-body formalisms and finite element modeling. The chain links were modeled as kinematically decoupled rigid bodies, which were interconnected by force elements. Sedlmayr and Pfeiffer [13] extended the previous work done by Srnik et al. [12] to include the effects of spatial orientation on the dynamics of CVT chain drives. The authors modeled the links and the pulleys as elastic bodies and also included pulley misalignment effects. Sattler [14] analyzed the mechanics of metal chain and V-belt considering both longitudinal and transverse stiffness of chain/belt, misalignment and deformation of pulley. The pulley deformation is modeled using a standard finite-element analysis. The pulley is assumed to deform in two ways, pure axial deformation and a skew deformation. The model was also used to study efficiency aspects of belt and chain CVTs. Lebrecht et al. [6] analyzed self-induced vibrations in a pushing V-belt CVT by using some highly simplified friction models. It was shown that the certain friction characteristics, especially those having negative gradient with respect to relative velocity, could induce self-excited vibration in the belt. The friction characteristic and the elasticity of the pulley sheaves also determined the working area where vibrations occurred.

Although the friction characteristic of the contacting surface inevitably plays a crucial role on CVT's performance, literature pertaining to the influence of friction characteristic on CVT dynamics is scarce [1,6-7]. Almost all the models, except a few, mentioned in the literature use Coulomb friction theory to model friction between the contacting surfaces of a CVT. However, depending on different operating (or loading) conditions and design configurations, the friction

characteristic of the contacting surface may vary. For instance, in case of a fully lubricated CVT, the friction characteristic of the contacting surface may bear a resemblance to the Stribeck curve [3] rather than to a continuous Coulomb characteristic. Moreover, very high forces in the contact zone may further lead to the conditions of elasto-plastic-hydrodynamic lubrication, which may yield a different friction characteristic. It has also been briefly reported [6] in literature that certain friction characteristics induce self-excited vibrations in the CVT system. However, it is not clear whether such phenomenon is an artifact of the friction model or the real behavior of the system. It is, thus, necessary to study the influence of different friction characteristics on the performance of transient-dynamic model of a chain CVT. It is also important to note that although an exact knowledge of the friction characteristic in a CVT system can only be obtained by conducting experiments on a real production CVT, these mathematical models give profound insight into the probable behavior that a CVT system exhibits under different operating conditions, which may be further exploited to design more efficient controllers.

The research reported in this paper focuses on the development of a detailed dynamic model of a chain CVT using multibody formalisms. Since excitation mechanisms exist due to impact and polygonal action of chain links in a chain CVT, it is necessary to model the chain CVT as a multibody system in order to accurately capture the dynamics arising from its discrete nature. The chain CVT model is developed using Pfeiffer and Glocker's theory [8] on multibody dynamics with unilateral contacts. Since it is experimentally cumbersome to measure exact friction characteristics of the contacting surfaces in a CVT system, different literature-based mathematical models of friction will be incorporated in the transient-dynamic CVT model in order to gain an insight into the influence of friction on the dynamic performance of a CVT. The goal is to understand the transient dynamic behavior of a chain CVT drive as chain links traverse the contacting arcs over the driver and driven pulleys and to also evaluate the system performance under different friction characteristics of the contact zone. The contact between the chain link and the pulley is modeled through different mathematical models of friction. The modeling analysis and the results corresponding to the chain CVT model are discussed in detail in the subsequent sections.

2. Modeling of a Chain CVT

As depicted in Figure 1, a chain CVT consists of two variable diameter pulleys connected to each other by a chain. The system is subjected to an input torque on the driver pulley and a resisting load torque on the driven pulley. The model captures various dynamic interactions between a chain link and the pulley as the link moves from the entrance to the exit of the pulley. The model development and analysis includes the following assumptions:

- The pulleys do not have any misalignment between them
- The chain links are rigid
- The interactions between the rocker pins of neighboring links and between a rocker pin and a plate can all be accounted for by modeling the chain link as a planar rigid body
- Negligible out-of-plane interaction of chain links
- Bending and torsional stiffness of the chain links are neglected

The modeling of various components of a chain-drive CVT is discussed subsequently.

Model of Chain Links:

The chain in the CVT is modeled link by link to account for its discrete structure. Each chain link represents a rigid body with three degrees of freedom in a plane (i.e. (x_c, y_c, θ)): two translations of the center of mass of the link and one rotation about an axis passing through the link's center of mass. The chain links are connected to each other by force elements which take into account the elasticity and damping of the links and joints. In case of contact between a link and a pulley, additional normal and tangential forces act on the bolt of the link and therefore on

the link. These contact forces correspond with the associated contact forces acting on the pulley. The force element is governed by a non-linear force-deformation law (like a hardening spring) in order to take the dynamic effects due to clearance between the links into account. Figure 3 and Figure 4 illustrate the free-body diagram of a chain link.

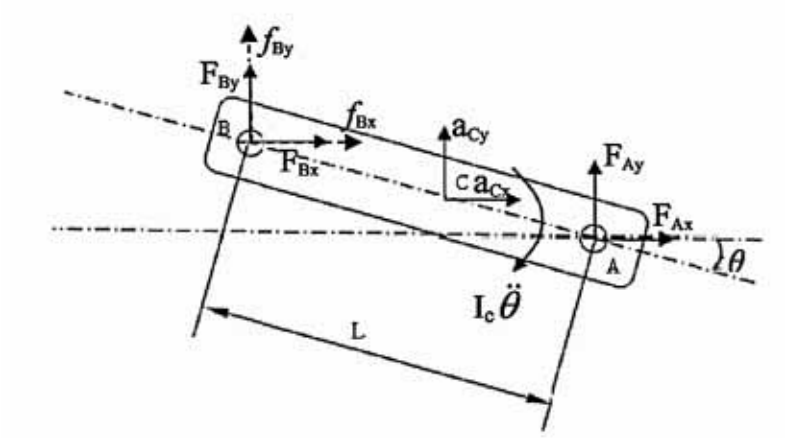

Fig. 2. Free body diagram of a chain link

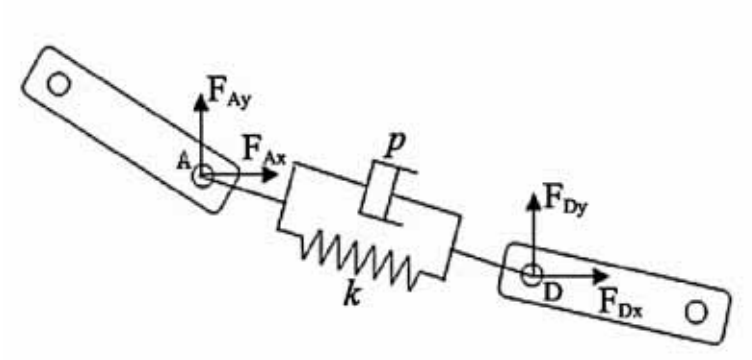

Fig. 3. Free body diagram of chain link interaction

It is to be noted that in Figure 3, the dotted arrows represent the forces (f_x and f_y,), which only arise when a chain link comes in contact with the pulley sheave. Using Newton-Euler equations, the equation of motion of a link not in contact with pulley can be written in matrix form, in terms of generalized coordinates, **q**, as:

$$\mathbf{J}^{\mathrm{T}}\begin{pmatrix} m\mathbf{E} & \mathbf{0} \\ \mathbf{0} & \mathbf{I}_{\mathrm{C}} \end{pmatrix}\mathbf{J}\ddot{\mathbf{q}} + \mathbf{J}^{\mathrm{T}}\begin{pmatrix} \mathbf{0} \\ \tilde{\boldsymbol{\Omega}}\mathbf{I}_{\mathrm{C}}\boldsymbol{\Omega} \end{pmatrix} = \mathbf{J}_{\mathrm{A,B}}^{\mathrm{T}}\begin{pmatrix} \mathbf{F} \\ \tilde{\mathbf{r}}_{\mathrm{A,B}}\mathbf{F} \end{pmatrix} \tag{1}$$

The generalized coordinates, q, for a link are (x_c, y_c, θ).The position vector of a point on the link from its center of mass, C, is denoted by **r**. The link mass and moment of inertia tensor about its center of mass is denoted by m and $\mathbf{I_c}$ respectively. **E** denotes the identity matrix. The Jacobian matrix, **J**, between the system coordinates and the configuration (or generalized) coordinates of a link at its center of mass can be obtained as,

$$\mathbf{v_C} = \begin{pmatrix} \dot{x}_C \\ \dot{y}_C \\ 0 \end{pmatrix}, \boldsymbol{\Omega} = \begin{pmatrix} 0 \\ 0 \\ \dot{\theta} \end{pmatrix}, \dot{\mathbf{q}} = \begin{pmatrix} \dot{x}_C \\ \dot{y}_C \\ \dot{\theta} \end{pmatrix}$$

$$\mathbf{J} = \begin{pmatrix} \mathbf{J_C} \\ \mathbf{J_R} \end{pmatrix} = \begin{pmatrix} \dfrac{\partial \mathbf{v_C}}{\partial \dot{\mathbf{q}}} \\ \dfrac{\partial \boldsymbol{\Omega}}{\partial \dot{\mathbf{q}}} \end{pmatrix} = \begin{pmatrix} 1 & 0 & 0 \\ 0 & 1 & 0 \\ 0 & 0 & 0 \\ 0 & 0 & 0 \\ 0 & 0 & 0 \\ 0 & 0 & 1 \end{pmatrix} \tag{2}$$

Similarly, Jacobian matrices in a link at the points of application of the active force **F** (A, B in the figure) can be obtained through the velocities of the corresponding points of the link, i.e., $\mathbf{J_A}$ can be obtained through an expression for velocity at point **A**, $\mathbf{v_A}$. The active forces, **F**, and the torques acting on a link due to these forces are obtained by computing the forces in springs and dampers of the force-elements connecting to that particular link. Now, summing (1) for all those links not in contact with the pulley will yield the following equation of motion for the multi-degree-of-freedom system,

$$\mathbf{M}(\mathbf{q}, t)\ddot{\mathbf{q}} - \mathbf{h}(\mathbf{q}, \dot{\mathbf{q}}, t) = \mathbf{0} \tag{3}$$

However, equation (3) does not take into account the contact force conditions between a link and the pulley. So, as the links come in contact with the pulley, they generate contact forces, which modify the equations of motion of the system. Hence, following analysis similar to [8], the equation of motion for all the links under unilateral contact conditions with the pulleys can be written as,

$$\mathbf{M}\ddot{\mathbf{q}} - \mathbf{h} - \left(\mathbf{W_N} + \mathbf{W_S}\hat{\boldsymbol{\mu}}_\mathbf{S}/\mathbf{W_T}\right)\begin{pmatrix} \boldsymbol{\lambda}_\mathbf{N} \\ \boldsymbol{\lambda}_\mathbf{T} \end{pmatrix} = \mathbf{0}$$

where

$$\hat{\boldsymbol{\mu}}_\mathbf{S} = \left\{-\mu_i\left(\dot{g}_{T_i}\right) sign\left(\dot{g}_{T_i}\right)\right\} \tag{4}$$

$\boldsymbol{\lambda}_\mathbf{N}$, $\boldsymbol{\lambda}_\mathbf{T}$ are the normal and the sticking constraint forces of the links that are in contact with the pulley and $\dot{\boldsymbol{g}}_{\boldsymbol{Ti}}$ is the tangential relative velocity between a link, i, and the pulley. $\mathbf{W_N}$ represents a matrix with coefficients of relative acceleration (in the normal direction) between links and pulley in the configuration space. $\mathbf{W_S}$ represents a matrix with coefficients of relative acceleration (in the tangential direction) between links and pulley in the configuration space when the links are slipping on the pulley sheave, whereas $\mathbf{W_T}$ represents a matrix with coefficients of relative acceleration (in the tangential direction) between links and pulley in the configuration space when the links are sticking to the pulley sheave. It is to be noted that the relative velocity and accelerations are computed at the contact points where links contact the pulley.

Model of Pulleys:

Each pulley is modeled as a rigid body with one degree of freedom i.e. the rotational degree of freedom (φ). A pulley is loaded with the frictional and normal forces acting between the rocker pins of the links and the pulley and also with an external moment. An input torque is applied to the driver pulley and a load torque on the driven pulley. Similar to equation (4), the equation of

motion of a pulley under unilateral contact conditions with the link is given by,

$$J_P\ddot{\varphi} = h_P - \left(\mathbf{W_{Np}} + \mathbf{W_{Sp}}\hat{\boldsymbol{\mu}}_S / \mathbf{W_{Tp}}\right)\begin{pmatrix}\boldsymbol{\lambda}_{\mathbf{Np}} \\ \boldsymbol{\lambda}_{\mathbf{Tp}}\end{pmatrix} \tag{5}$$

The term, h_P, accounts for the moment contributions from the input and load torques on the pulleys. The terms, $\mathbf{W_{NP}}$, $\mathbf{W_{SP}}$, $\mathbf{W_{TP}}$ are analogous to the terms, $\mathbf{W_N}$, $\mathbf{Ws}$, $\mathbf{W_T}$ in equation (4).

Occasionally, it has been observed [2,12-17] that the variation of local groove width caused by the elastic deformation of the pulleys significantly influences the thrust ratio and slip behavior of a belt/chain CVT. However, since the primary goal of this research was to study the influence of friction characteristic on CVT dynamics, a detailed finite-element modeling of pulley sheaves was evaded. Hence, instead of a detailed finite-element formulation of pulley sheaves, simple trigonometric functions (as outlined in [2, 16-17]) are used to describe the varying pulley groove angle and the local elastic axial deformations of the pulley sheaves. Figure 5 depicts the model for pulley deformation. The following equations describe pulley deformation effects in Figure 5:

$$\beta = \beta_O + \frac{\Delta}{2}\sin\left(\varsigma - \theta_c + \frac{\pi}{2}\right) \tag{6}$$

The angular location of a chain link over driver and driven pulley wrap is denoted by ζ in equation (6). Using this approximation for the sheave angle deformation, the pitch radius of the chain link in the deformed pulley sheave can be easily computed. The amplitude of the variation in the pulley groove angle, Δ, is always much smaller than unity, however, it is not constant during speed ratio changing phases due to variation in the pulley axial (clamping) forces. Sferra *et al.* [16] proposed the following approximate correlations for the variation Δ and the center of the pulley wedge expansion θ_c in terms of the transmitted torque τ, and the chain pitch radius on driver and driven pulleys, r and r' respectively.

$$\Delta = \frac{0.00045\tau}{\left(\frac{r}{r'}\right)^{0.55}}$$
$$\theta_c = \frac{\pi}{3}\frac{r}{r'} + \frac{23\pi}{180} \tag{7}$$

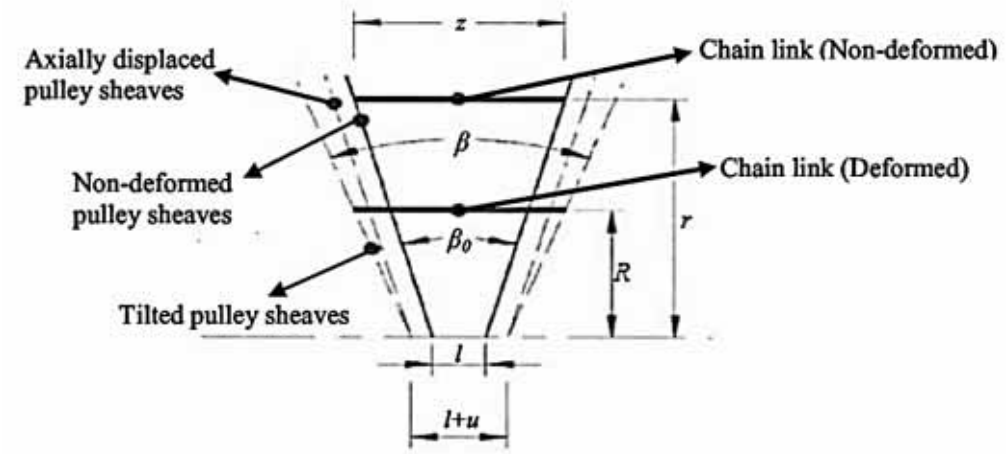

Fig. 5. Pulley Deformation Model [2

Model of Link-Pulley Contact:

A chain link contacts a pulley at the ends of a rocker pin. As the plates move, the rocker pins of adjacent links also interact with each other. Assuming negligible dynamic interaction between a pair of rocker pins, these rocker pins are modeled as a single bolt. So, every link is associated with one bolt through which it contacts the pulley sheaves. The bolt is represented as a linear massless spring. The contact planes of the bolts are the end faces of the springs. The surfaces of the bolt are loaded with the normal and frictional contact forces. Figure 6 illustrates the free diagram for the interactions between the bolt and a pulley. In this figure, $\mathbf{F_r}$ and $\mathbf{F_t}$ represent the components of the resultant friction force vector $\mathbf{F}_f$ between a chain link and the pulley, which act in the plane of the pulley sheave, and **N** is the normal force between the link and the pulley.

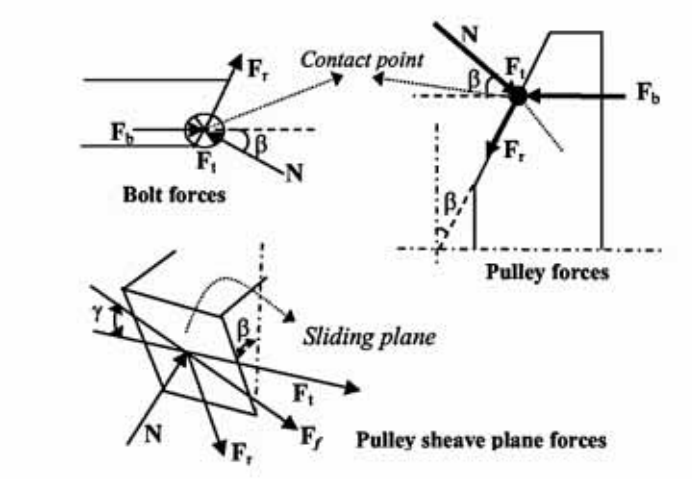

Fig. 6. Link-Pulley Contact Description

It is necessary to quantify the bolt spring force, F_b, in order to derive the contact forces. The bolt force depends on the bolt length l_b and stiffness K_b as well as on the local distance of the pulley's surfaces z. Since the pulley sheaves also bend, additional axial width variation (refer Figure 6) affects the bolt force. So, the bolt force, F_b, can be written as:

$$F_b = \begin{cases} K_b\left(l_b - z - u\right) \forall \left(z+u\right) \le l_b \\ 0 \qquad\quad \forall \left(z+u\right) > l_b \end{cases} \tag{8}$$

It is to be noted that the chain link slips in the plane of the pulley sheave. The slip angle, γ, defines the plane in which the friction force acts. It is the angle which the resultant friction force vector, $\mathbf{F}_f$, makes with the tangential direction vector to the pulley. So, in order to get the friction force vector, it is crucial to keep a track of the relative velocity vector between the chain link and the pulley.

Modeling of friction between a link and the pulley:

Almost all the models, except the few mentioned in the literature, use classical Coulomb-Amonton friction law to model friction between the contacting surfaces of a CVT. The friction phenomenon described by this law is inherently discontinuous in nature. It is common engineering practice to introduce a smoothening function to represent the set-valued friction law. However, certain friction-related phenomena like chaos, limit-cycles, hysteresis, etc., are neither easy to detect nor easy to explain on the basis of classical Coulomb-Amonton friction theory. Since it is difficult to monitor friction experimentally during the running conditions of a complex nonlinear system (e.g. a CVT), mathematical models of friction give insight into the different dynamic maneuvers that a system can undergo.

It is evident that equations (4) and (5) possess time-varying structure due to the possible transitions between stick and slip phases of the contact. However, without significant loss of accuracy [12], it is possible to evade this time-variance in the system by assuming the friction between the bolt of the chain link and the pulley to be approximated by a smooth nonlinear function. Two different mathematical models are embedded into the multibody model of chain CVT in order to capture the friction between the link and the pulley. Figure 7 depicts the friction characteristics described by these mathematical models.

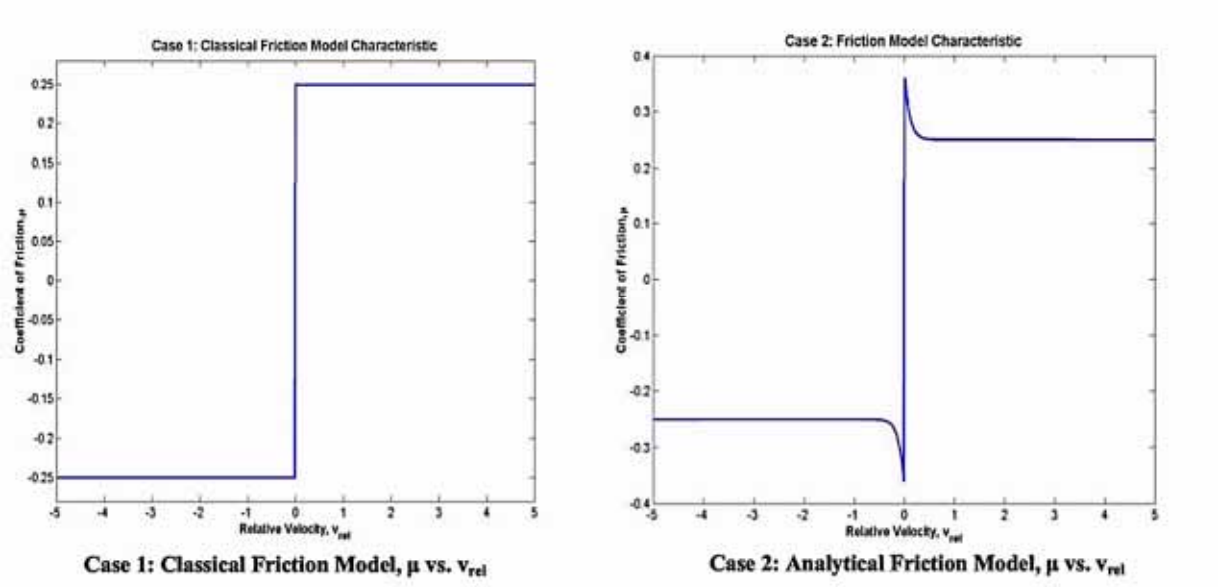

Fig. 7. Friction characteristics for the contact zone

The coefficient of friction between the link and the pulley is governed by the following relationship:

$$\textbf{Case 1}: \quad \mu = a + (\mu_o - a)\left(1 - e^{-|v_{rel}|/b}\right)$$

$$\textbf{Case 2:} \quad \mu = \mu_o \left(1 - e^{\kappa|v_{rel}|}\right)\left(1 + (\sigma - 1)e^{-\chi|v_{rel}|}\right) \tag{9}$$

The coefficient of friction mentioned in Case 1 describes the classical Coulomb-Amonton friction law which aptly captures the dynamics associated with kinetic friction and is most commonly referenced in literature. However, the coefficient of friction mentioned in Case 2 is more detailed as it not only captures the dynamics associated with kinetic friction, but also captures the dynamics associated with stiction- and Stribeck- effects (which are prominent under dry and lubricated contact conditions respectively).

3. Results and Discussion

A CVT system is continually subjected to torques from both the engine and the final drive inertias. The engine creates an input torque condition on the driver pulley and the final drive exerts a load torque on the driven pulley. The modeling development was done on the MATLAB/Visual C++ platform. The Runge-Kutta method is used to integrate state equations in order to get time histories of the system states. The simulation of a chain-CVT model starts off with an initial condition of rest and a specific design configuration and computes different dynamic performance

indices i.e. axial forces, angular velocities, tension, etc. The driver pulley is subjected to a high input torque (200 Nm) whereas a low resisting load torque (100 Nm) is applied to the driven pulley. The results corresponding to two different friction characteristics are discussed subsequently.

Figure 8 depicts the time histories of the distance of a chain link from the center of driver pulley for both the cases. The variation in link distance is computed by tracing the position of a link from the center of the driver pulley as the link traverses the different section of the chain CVT, i.e. the free-strands, the driver pulley, and the driven pulley. It can be readily observed from the figure that the chain-link pitch radius on the driver pulley is not the same for all the cases. Figure 9 depicts an exploded view of the variation in the pitch radius of the chain link as it traverses the driver pulley wrap.

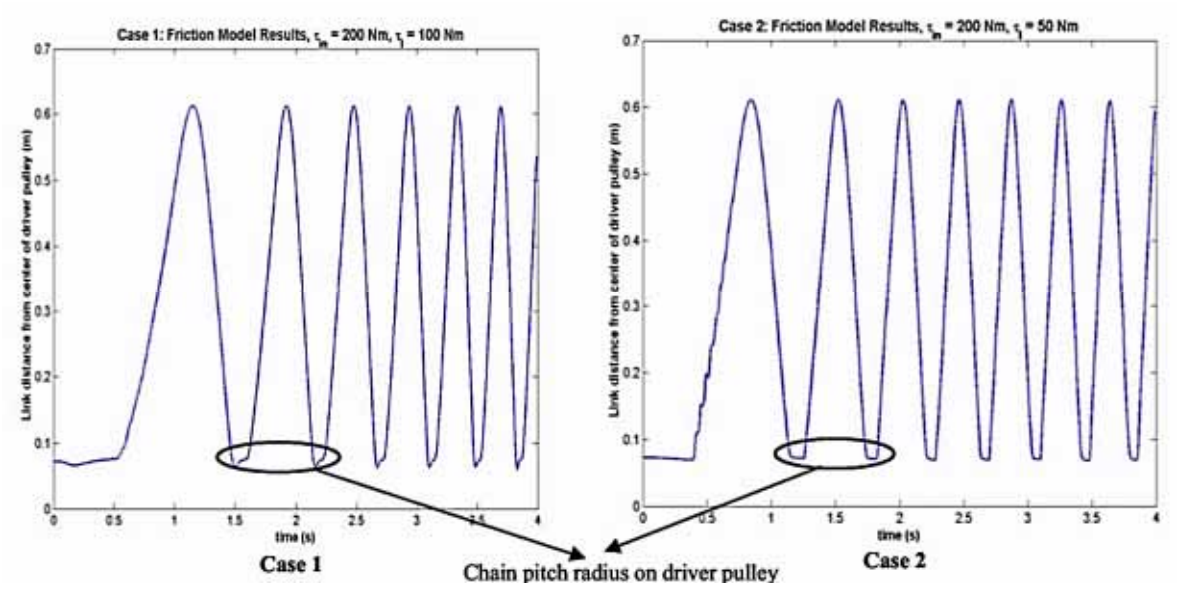

Fig. 8. Time history of link distance from center of driver pulley

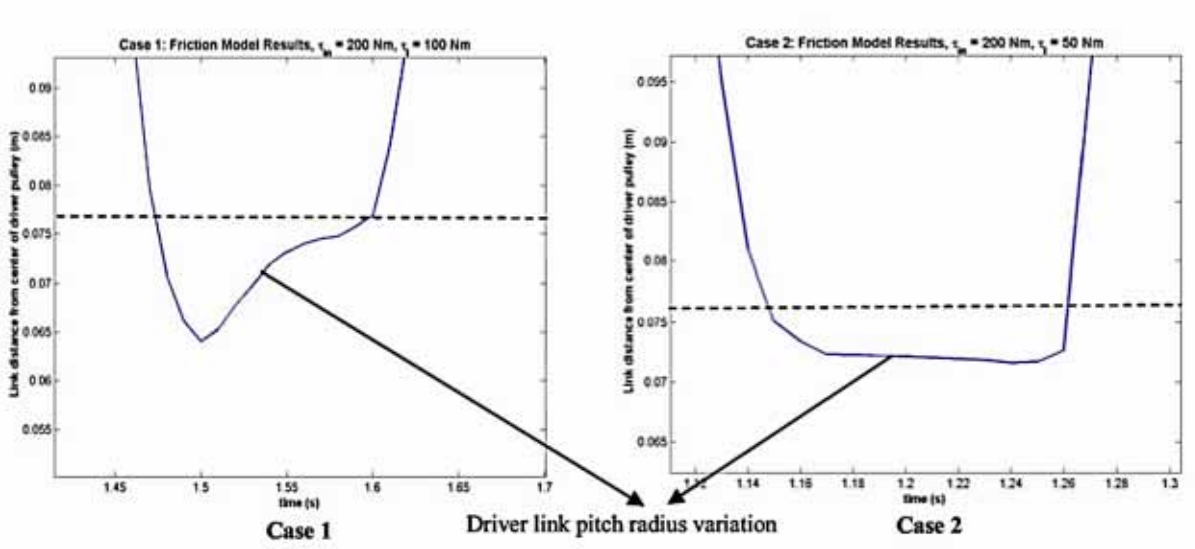

Fig. 9. Exploded view of chain link pitch radius on driver pulley

As the chain link enters the driver pulley groove, the chain pitch radius decreases. This phenomenon can be attributed to the wedging action between the link and the pulley. However, as

the link traverses the pulley wrap, the chain pitch radius increases till the link exits the pulley. This can be attributed to the drop in the tensile force of the link as it moves from the entrance to the exit of the driver pulley. It can be noted from the figure that the chain links travel faster in case 2 than in case 1 owing to the presence of a lower resisting load torque (50 Nm) on the driven pulley for case 2. It was observed (refer Figure 10) that a chain CVT under the presence of a friction characteristic governed by case 2 was unable to sustain a higher load torque of 100 Nm, which was contrary to the load carrying capacity predicted by the classical continuous Coulomb friction law (i.e. under case 1). Moreover, owing to larger normal force generation in case 1, the radial path-traversed by a chain link in the driver pulley groove is greater in this case than in case 2. A chain link contacting the driven pulley also shows complementary behavior in the entry and exit phases of its motion.

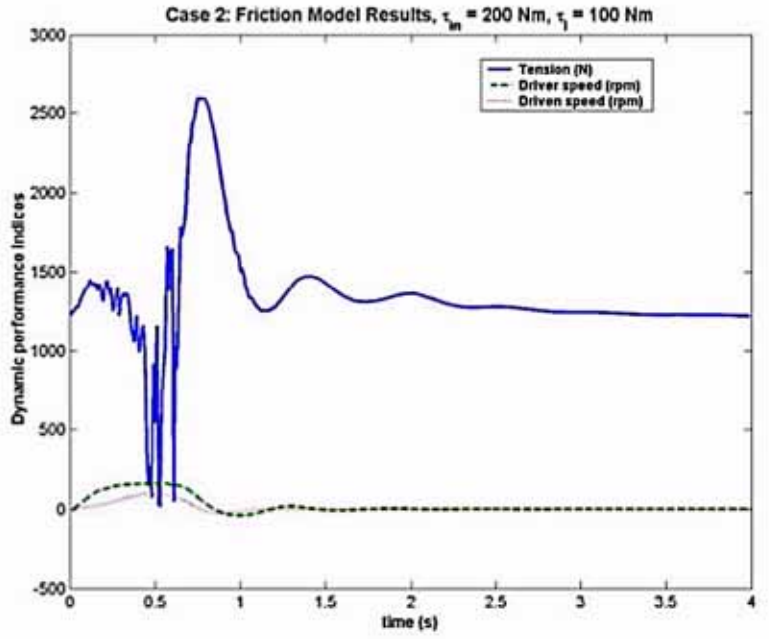

Fig. 10. Time histories of dynamic performance indices (Tension and pulley speeds) Case 2: Input = 200 Nm, Load = 100 Nm

Figure 11 illustrates the time histories of the normal force between a chain link and the pulley for both the cases. Whenever a chain link comes in contact with the pulley, it exerts a normal force on the sheave, which tends to move the pulley sheaves apart. The pulley normal force has a non-uniform distribution over the contact arc. The normal force increases from the entrance to the exit of the driven pulley, which is in consonance with the observations made by Ide *et al.* [4] and Pfeiffer *et al.* [12]. Moreover, the normal force generated between the driver pulley and the chain link is higher than the normal force generated between the link and the driven pulley. As the chain link wedges into the pulley groove, a significant amount of radial friction force is generated to prevent the inward radial motion of the chain link. Since during the wedging the pitch radius of the chain link decreases on the driver pulley (as depicted in Figure 9), the link exerts a large normal force on the pulley in order to generate enough torque to compensate for the resisting load on the driven pulley. Since the variations in the pitch radius of the chain on the driven pulley are higher than those over a driver pulley, an adequate amount of normal force between the link and the pulley generates enough friction torque to meet the resisting load torque. It can also be observed from the figure that the normal force generated is lower for case 2 than for case 1 because of the lower load torque requirements on the driven pulley for case 2 as well as due to the presence of lubrication-related dynamic effects.

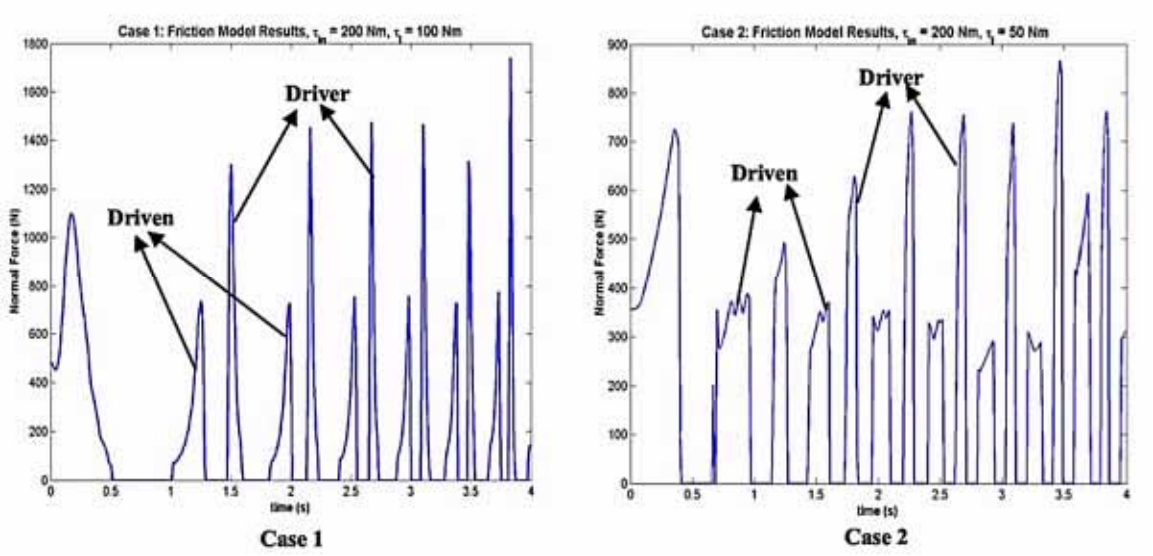

Fig. 11. Time history of normal force

Since one of the pulley sheaves is movable, the chain link is capable of exhibiting both-tangential and radial motions when it traverses the pulley wrap angle. Consequently, a friction force is generated in the sliding plane, which opposes the relative velocity between the chain link and the pulley. Knowing the sliding direction and the sheave angle, the friction force in the sliding plane can be readily decomposed into radial and tangential components. Figure 12 illustrates the time histories of the tangential friction force for both the cases. The tangential friction force acts as the transmitting force and causes the variations in the tensile force of the chain links. It can be observed from the figure that the tangential friction force between the driver pulley and the link is in anti-phase to the tangential friction phase between the driven pulley and the link. This relationship, in fact, aptly describes the energy transfer interactions between the chain link and the pulleys. It is to be noted that the transmitting force in case 2 is higher than in case 1. Since chain links traverse greater radial path in case 1 than in case 2, the transmitting force required to overcome the resisting load torque is not high enough for case 1. It is to be noted from the time histories of normal force and friction force that the chain CVT system exhibit greater wedging losses in case 2 owing to noisy entrance and exit dynamics over the pulley wraps.

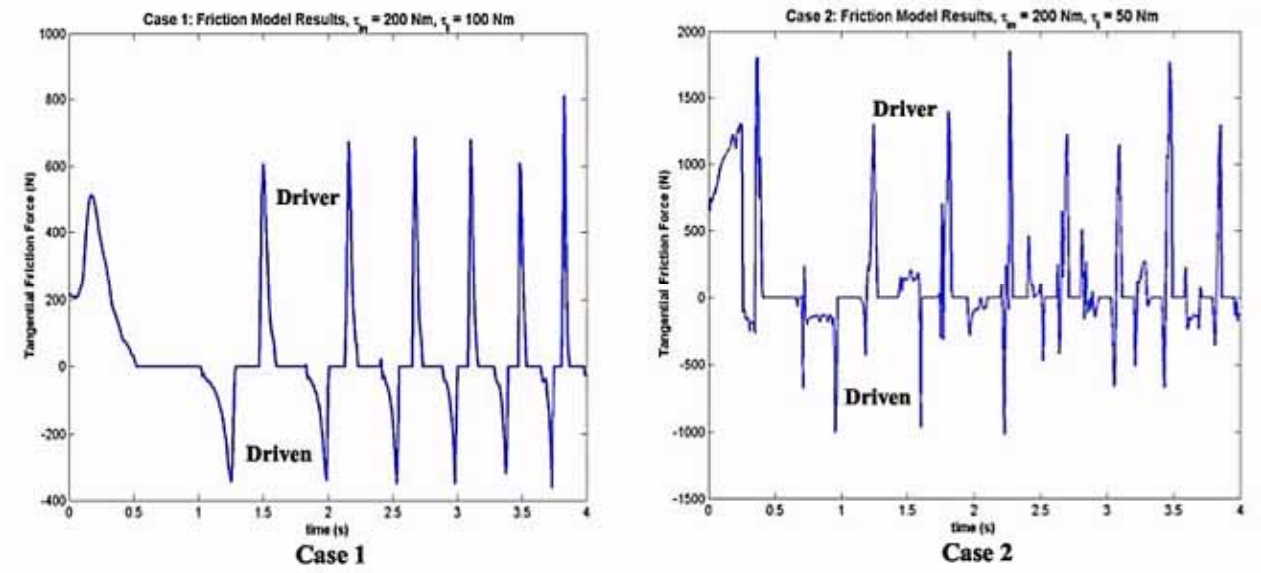

Fig. 12. Time history of tangential friction force

Figure 13 illustrates the time histories of the tensile force in the chain links for both the cases. It is to be noted that the tensile force in the chain links drops as the links traverse the driver pulley wrap from the inlet to the exit of the pulley. On the contrary, the tensile force increases as the links traverse the driven pulley wrap from the inlet to the exit of the pulley. Moreover, with passage of time, the tensile force in the chain links increases. It can also be noted from the figure that the link tension exhibits significant variations as the link passes through the entry and exit regions of the pulleys for a CVT system with friction described by case 2. This not only degrades the system performance, but also induces irregular behavior in the system, which might be difficult to control. Moreover, since the transmitting force required to meet the load torque is higher for case 2, the tensile force in the chain links with friction described by case 2 is higher is in comparison to the tensile force generated in case 1. It is plausible from the plots that a CVT system with the classical continuous Coulomb friction characteristic (i.e. case 1) is able to transmit torque much more smoothly than a CVT system with friction characteristic governed by case 2.

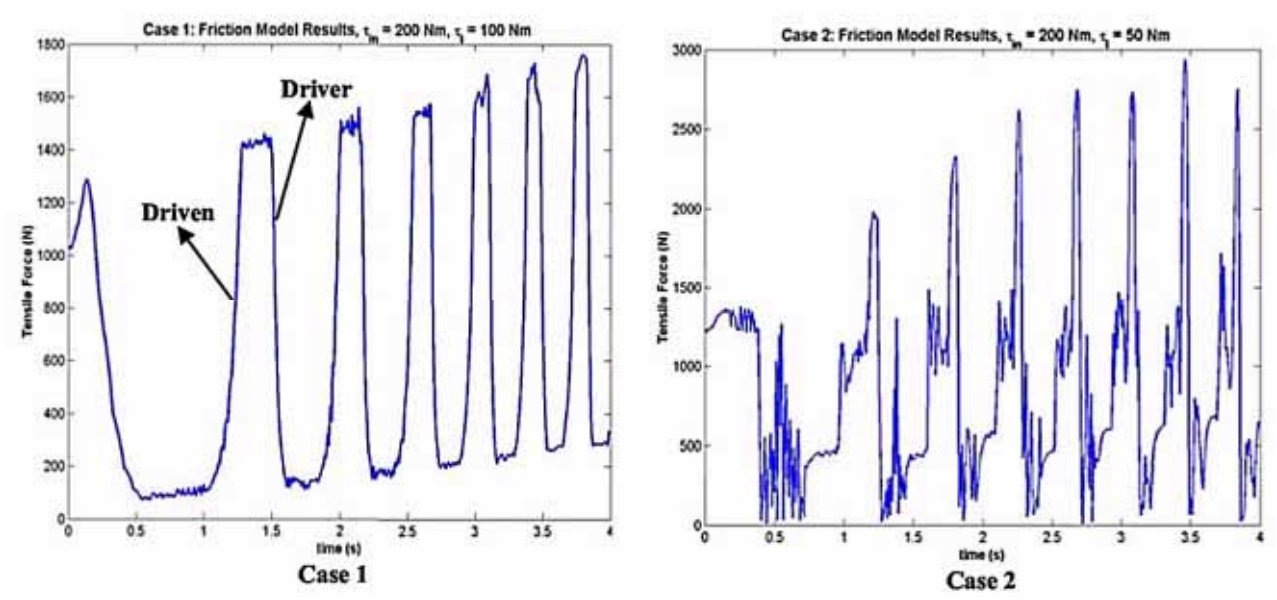

Fig. 13. Time history of tensile force in the chain links

As mentioned previously, the pulleys are subjected to torque-loading conditions. An input torque is applied to the driver pulley, whereas the driven pulley is subjected to an opposing load torque. The links and the pulleys start off from a zero initial velocity configuration, and the angular speeds of the pulleys are recorded during the simulation. Figure 14 illustrates the time histories of the pulley angular speeds. It can be inferred from the plots that the CVT system entails greater losses in case 2 than in case 1, as, in spite of a low load torque of 50 Nm, it is not able to generate enough friction torque to rev up the driven pulley. However, there is a greater difference between the driver and driven pulley speeds for case 1 than for case 2. This can be attributed to the greater radial penetration of chain links in the pulley groove under the friction characteristic described by case 1. Consequently, the friction torque on the driver pulley decreases (thereby, increase in driver pulley speed), whereas it increases on the driven pulley (thereby, increasing friction torque to oppose the load on driven pulley).

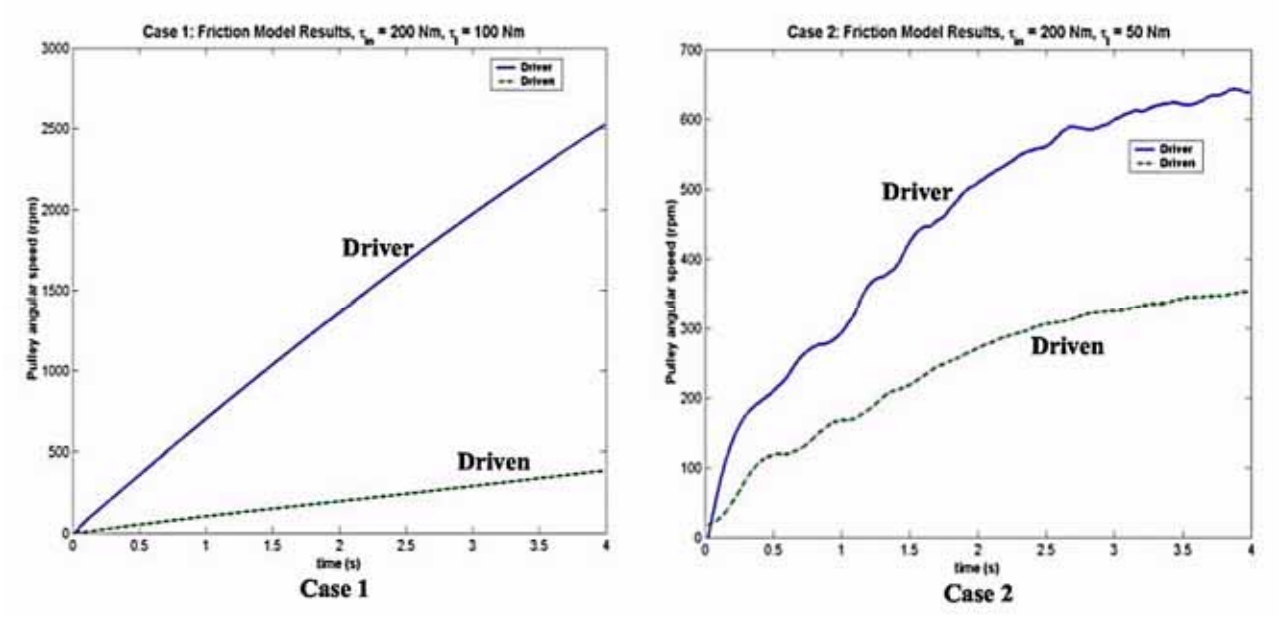

*Fig. 14. Time history of pulley angular speeds **4.***

Conclusions

The paper outlined a detailed planar multibody model of a chain CVT under the influence of two different friction characteristics that describe the friction between the chain link and the pulley. A chain CVT falls under the category of friction-limited drives as its performance and torque capacity rely significantly on the friction characteristic of the contact patch between the chain and the pulley. Depending on different operating (or loading) conditions and design configurations, the friction characteristic of the contacting surface may vary. For instance, in case of a fully lubricated CVT, the friction characteristic of the contacting surface may bear a resemblance to the Stribeck curve rather than to a continuous Coulomb characteristic. It is quite feasible to have a lubricated contact in a belt/chain CVT in order to reduce wear and thermal effects.

With an aim to understand friction-related dynamics, two different mathematical models of friction were incorporated to describe friction between the link and the pulley. The friction characteristic in case 2 is able to capture not only the kinetic friction effects (as in case 1), but also the effects similar to stiction and boundary-lubrication. It was observed that the torque carrying capacity of the CVT system lowered under the presence of friction characteristic as described by case 2. Moreover, the chain CVT entails greater losses from noise, vibration, and wedging of the chain links in case 2 than in case 1. The variation in the transmission ratio is also higher for case 1 than for case 2. It is evident from the results that CVT, being a highly nonlinear system, is capable of exhibiting varied performance under different friction characteristics of the contact zone between the link and the pulley. It is also plausible for the system to undergo chaoticity which not only hampers the torque transmission, but also makes it difficult to be controlled. So, the performance of a CVT can vary drastically from the condition of dry friction to a fully-lubricated condition.

A more accurate analysis of the torque transmissibility of a chain CVT system can be done by modeling the links as elastic bodies, accounting for spatial orientation of the chain links (using a spatial model), and by developing a finite element model for elastic deformations in the pulley sheave. However, since the primary goal of this research was to study the influence of friction-related dynamics on the performance of chain CVT, a planar chain CVT with an approximate

pulley bending model suffices the purpose. It is also important to note that although an exact knowledge of the friction characteristic in a CVT system can only be obtained by real-time monitoring of the contact patch dynamics in a production CVT, these mathematical models give profound insight into the probable behavior that a CVT system exhibits under different operating conditions, which may be further exploited to design efficient CVT controllers, to analyze the noise and vibration behavior of a CVT-loaded powertrain or vehicle, etc.

Acknowledgements

This research was supported by the Automotive Research Center (ARC), a U.S. Army TACOM Center of Excellence for Modeling and Simulation of Ground Vehicles. The support and interest of our sponsors is gratefully acknowledged.

References

[1] Carbone, G., Mangialardi, L., Mantriota, G., *EHL visco-plastic friction model in CVT shifting behaviour,* International Journal of Vehicle Design, Vol. 32, Nos. 3/4, pp. 333-357, 2003.

[2] Carbone, G., Mangialardi, L., Mantriota, G., *The Influence of Pulley Deformations on the Shifting Mechanism of Metal Belt CVT,* Trans. ASME, Journal of Mechanical Design, Vol. 127, pp. 103-113, 2005.

[3] Canudas de Wit, C., Olsson. H., Astrom, K. J., Lischinsky, P., *Dynamic friction models and control design,* Proceedings of the 1993 American Control Conference, pp. 1920-1926, San Francisco, California, USA, 1993.

[4] Ide, T., Tanaka, H., *Contact Force Distribution between Pulley Sheave and Metal Pushing V-belt*, Proceedings of CVT 2002 Congress, VDI-Berichte, Vol. 1709, pp. 343-35, 2002.

[5] Kobayashi D., Mabuchi Y., Katoh Y., *A Study on the Torque Capacity of a Metal Pushing V-Belt for CVTs,* SAE Transmission and Driveline Systems Symposium, SAE Paper No. 980822, 1998.

[6] Lebrecht, W., Pfeiffer, F., and Ulbrich, H., *Analysis of self-induced vibrations in a pushing V-belt CVT,* 2004 International Continuously Variable and Hybrid Transmission Congress, Paper No. 04CVT-32, September 23-25, San Francisco, USA, 2004.

[7] Micklem, J. D., Longmore, D. K., Burrows, C. R., *Modelling of the Steel Pushing V-belt Continuously Variable Transmission,* Proceedings Inst. Mech. Engineers, Part C, Vol. 208, pp 13-27, 1994.

[8] Pfeiffer, F., Glocker, C., Multibody Dynamics with Unilateral Contacts, *Wiley-Interscience,* ISBN 0471155659, 1996.

[9] Srivastava, N., Haque, L, *On the transient dynamics of a metal pushing V-belt CVT at high speeds,* International Journal of Vehicle Design, 37(1), pp. 46-66, 2005.

[10] Srivastava, N., Haque, I. U., *On the operating regime of a metal pushing V-belt CVT under steady state microslip conditions,* 2004 International Continuously Variable and Hybrid Transmission Congress, Paper No. 2004-34-2851 (04CVT-11), San Francisco, USA, September 23 - 25, 2004.

[11] Srivastava, N., Blouin, V. Y., Haque, I. U., *Using Genetic Algorithms to Identify Initial Operating Conditions for a Transient CVT Model,* 2004 ASME International Mechanical Engineering Congress, Paper No. IMECE2004-61999, Anaheim, CA, USA, November 13-19, 2004.

[12] Srnik, J. and Pfeiffer, F., *Dynamics of CVT chain drives,* Int. J. of Vehicle Design, 22(1/2), pp. 54-72, 1999.

[13] Sedlmayr, M., Pfeiffer, F., *Force reduction in CVT Chains,* Int. J. of Vehicle Design, 32(3/4), pp. 290-303, 2003.

[14] Sattler, H., *Efficiency of Metal Chain and V-belt CVT,* Int. Congress on Continuously Variable Power Transmission CVT' 99, pp. 99-104, Eindhoven, The Netherlands, September 16-17,1999.

[14] Sorge, F., *Influence of Pulley Bending on Metal V-Belt Mechanics,* In Proceedings of International Conference on Continuously Variable Power Transmission, Japanese Society of Automotive Engineers, Paper No. 102 (9636268), pp. 9-15, Yokohama, Japan, September 11-12, 1996.

[15] Sferra, D., Pennestri, E., Valentini, P. P., and Baldascini, F., *Dynamic Simulation of a Metal-Belt CVT under Transient Conditions,* Proceedings of the DETC02, 2002 ASME Design Engineering Technical Conference, Paper No. DETC02/MECH-34228, Vol. 5A, pp. 261-268, Montreal, Canada, September 29-October 2, 2002.

[16] Srivastava, N., Yi, M., Haque, I. U., *Influence of clearance on the dynamics of chain CVT drives,* 2006 ASME International Mechanical Engineering Congress, Paper No. IMECE2006-14059, Chicago, IL, USA, November 5-10, 2006 (submitted).